MODELING OF SURFACE DEFORMATION IN AN ELECTROMAGNETICALLY STIRRED METALLIC MELT

J. Partinen*, N. Saluja*, J. Szekely*, and J.K. Kirtley, Jr.**

* Dept. of Mat. Sci. and Eng., MIT.
** Dept. of Electrical Eng. and Computer Sci., MIT.

Abstract

A computational model was developed to calculate the velocities and free surface deformation in a turbulent electromagnetically stirred metallic melt. The predictions were compared with observations made on a laboratory-scale system, and the free surface velocities were extracted from data obtained through high-speed video photography.

Introduction

The interaction between electromagnetic forces and fluid flow occurs frequently in materials processing operations: induction stirring in continuous casting, electromagnetic braking, the use of magnetic fields to suppress convection in crystal growth, and many others may be cited as representative examples [1-4]. Newer applications include melt shaping, meniscus control, and electromagnetic atomization.

This growing interest in electromagnetic phenomena is reflected by the extensive literature of this technology, notable examples of which include several textbooks [5-7] and symposium proceedings [8].

As part of the research effort aimed at studying the magnetohydrodynamic (MHD) phenomena in metals processing, extensive work has been carried out to model the fluid flow field produced by the application of the electromagnetic forces. However, in the vast majority of the work reported up to the present, free surface phenomena received very little attention, notwithstanding the fact that in many applications pertaining to the electromagnetic stirring of continuous casting systems, the deformation of the free surface disturbances may play an important role in affecting product quality.

Recent work in the authors' laboratory has addressed this problem from a theoretical modeling viewpoint [9-13] but as yet little or no experimental confirmation is available.

The main purpose of the present paper is to present a set of experimental measurements aimed at determining the free surface deformation in a physical model system, which is being stirred electromagnetically, so as to provide a test of the previous models.

Theoretical

The fluid flow phenomena in an electromagnetically stirred system can be represented by the equation of mass conservation, equations of motion for a turbulent system, and an appropriate turbulence model [14] to calculate the Reynolds stresses. In this model, the eddy viscosity is evaluated using the k-ε model [15]; k (turbulent kinetic energy) and ε (viscous dissipation) are in turn evaluated by their individual transport equations.

Equation of mass conservation for incompressible fluids:

$$\vec{\nabla} \cdot \bar{\vec{u}} = 0 \qquad (1)$$

where $\bar{\vec{u}}$ is the time-averaged turbulent velocity.

Equation of motion for turbulent systems:

$$\rho\frac{D\vec{\bar{u}}}{Dt} = -\vec{\nabla}p - \vec{\nabla}\cdot\underline{\underline{\tau}}^{l} - \vec{\nabla}\cdot\underline{\underline{\bar{\tau}}}^{t} + \rho\vec{F}_{EM} \qquad (2)$$

where $D(\vec{\bar{u}})/Dt$ denotes the substantial derivative, p is the pressure, $\vec{F}_{EM}$ is the electromagnetic body force per unit volume, $\underline{\underline{\tau}}^{l}$ is the laminar stress tensor, $\underline{\underline{\bar{\tau}}}^{t}$ is the Reynolds stress term that is time-averaged, and ρ is the mass-density of the melt. The equations of motion are solved for the three principal directions of the cylindrical coordinate system: radial (r), axial (z), and azimuthal (θ).

The turbulent and laminar viscous terms may be combined to yield an effective dynamic viscosity μ_{eff}, which is the sum of the laminar (μ_l) and turbulent (μ_t) viscosities:

$$\vec{\nabla}\cdot\underline{\underline{\tau}}^{l} + \vec{\nabla}\cdot\underline{\underline{\bar{\tau}}}^{t} = -\vec{\nabla}\cdot\left[(\mu_l + \mu_t)\vec{\nabla}\vec{\bar{u}}\right] = -\vec{\nabla}\cdot\left(\mu_{eff}\vec{\nabla}\vec{\bar{u}}\right) \qquad (3)$$

The evaluation of μ_{eff} is enabled by the use of the k-ε model, where the turbulent viscosity is calculated by a relationship of the type:

$$\mu_t = \rho c_\mu \frac{k^2}{\varepsilon} \qquad (4)$$

where $C\mu$ is an empirical constant (= 0.09 in our computations). The equations governing k and ε, along with the associated boundary conditions, are readily available in literature [15], and are not reproduced in this paper.

The electromagnetic force field is calculated by the use of Maxwell's equations using the assumptions that the magnetic field is quasi-static, harmonic, and that the material characteristics are linear. In addition, it is assumed that the liquid metal is acted on by a time-averaged force, $\vec{F}_{EM}$.

Continuity of the magnetic flux:

$$\vec{\nabla}\cdot\vec{B} = 0 \qquad (5)$$

Ampere's law:

$$\vec{J} = \vec{\nabla} \times \vec{H} \tag{6}$$

Faraday's law:

$$\vec{\nabla} \times \vec{E} = -\frac{\partial \vec{B}}{\partial t} \tag{7}$$

Ohm's law for moving media:

$$\vec{J} = \sigma\left[\vec{E} + \left(\vec{u} \times \vec{B}\right)\right] \tag{8}$$

where $\vec{E}$ is the electric field, $\vec{H}$ is the magnetic field strength, $\vec{B}$ is the magnetic flux density, and $\vec{J}$ is the induced current density.

The electromagnetic force per unit volume of the fluid is given by the vector product of $\vec{J}$ and $\vec{B}$.

$$\vec{F}_{EM} = \vec{J} \times \vec{B} \tag{9}$$

The volumetric, time-averaged electromagnetic force components are given by the following expression [16]:

Radial component:

$$\overline{F_r} = -\frac{1}{8} B_o^{\,2} \left(\omega - \frac{u_\theta}{r}\right)^2 \sigma^2 \mu_o r^3 \tag{10}$$

Azimuthal component:

$$\overline{F_\theta} = \frac{1}{2} B_o^{\,2} \left(\omega - \frac{u_\theta}{r}\right) \sigma r \tag{11}$$

where B_0 is the amplitude of the radial component of $\vec{B}$ inside the stirrer, σ is the electrical conductivity, μ_0 is the magnetic permeability, u_θ is the azimuthal velocity, ω is the angular velocity of the applied coil current, and r is the radial coordinate.

The equations are solved using a commercially available code, Flow-3D, wherein the electromagnetic body forces are introduced as body acceleration terms. The free-surface is tracked using the volume-of-fluid (VOF) method [17].

The calculation is performed on an axi-symmetric r - z mesh with 45×60 uniform grids. The hardware used is a VaxStation 3100 M38, and it takes approximately 130 hours of CPU time to perform a simulation which represents a real time of ~3 seconds.

Experimental

The experimental apparatus (Figure 1) consists of the electromagnetic stirrer (a helical coil wound on an armature [18]), along with peripheral electrical apparatus to control the current-voltage characteristics of the power supply as well as the frequency of the coil current. In addition, adequate quantities of coolants (silicone oil for the stirrer, and water for the oil system) have to be pumped through the system to prevent overheating. The variable-frequency drive enables the frequency to be varied from 2 to 60 Hz.

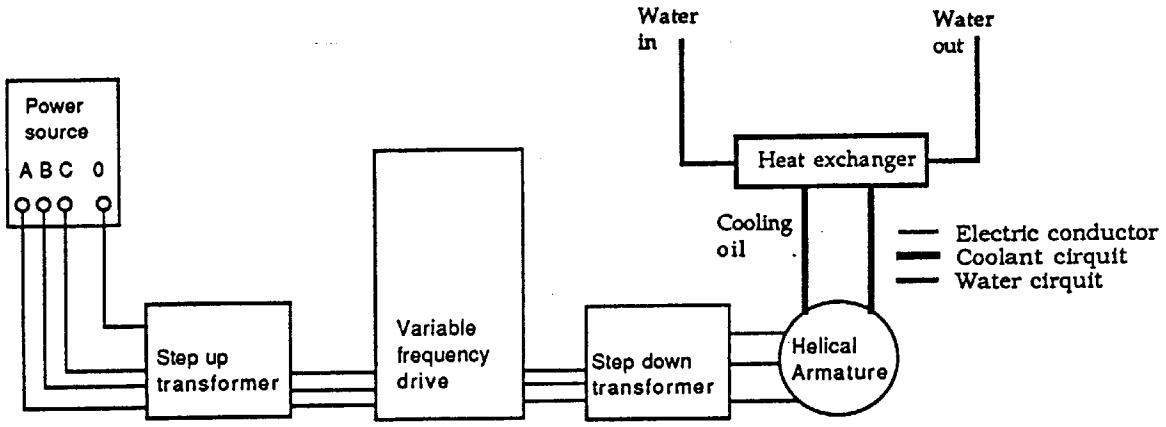

Figure 1. Schematic description of the stirring system

The stirrer is rated at 60 kVA, and is capable of producing fields in the range of ~ 1000 gauss. In this work, however, fields of the range of 450 G were employed, which is sufficient to produce rather severe free surface deformation in a Wood's metal system contained in a clay-bonded graphite crucible (inner

diameter: 90 mm). The properties of the melt are given in Table 1 [9]. The magnetic field measurements were affected by the use of Hall probes and search-coils. The field losses due to the crucible are found to be negligible.

Table I. Properties of the Wood's metal [7]

50Bi–25 Pb–12.5 Sn–12.5 Cd
(Bi:Pb:Sn:Cd :: 4:2:1:1)
Melting Point: 70 °C

ρ	Density	8.37×10^3 kg m^{-3}
μ	Molecular viscosity	2.29×10^{-3} kg m^{-1} s^{-1}
σ	Electrical conductivity	9.0×10^5 Ω^{-1} m^{-1}
c_p	Specific heat	1.255×10^2 J kg^{-1} K^{-1}
k	Thermal conductivity	1.405×10^1 J m^{-1} s^{-1} K^{-1}
β	Thermal expansion coefficient	1.0×10^{-4} K^{-1}

The surface velocity measurements are made using high-speed video photography, and a speed of 500 frames/second is chosen to analyze the surface velocities and study the particle engulfment in the melt.

The magnitude of the free surface deformation is measured using a X-Y translation platform, with a Z-translation pin. The fluid heights are measured along the wall and the the centerline of the crucible.

Results and discussion

Figure 2 shows the measured values of the azimuthal (B_θ) and radial (B_r) components of the magnetic flux density along the axial length of the stirrer. It is seen from the bell-shaped curves that the B-values have a maximum at the center of the stirrer coil, and decrease towards the edges of the coil. ΔZ here refers to the distance from the top of the coil. Figure 3 depicts the measurement technique employed to measure the free surface deformation. The total free surface deformation is seen to be the sum of ΔW (height at the crucible wall to 'rest' or level of the un-stirred melt) and ΔC (height from 'rest' level to height at the crucible centerline).

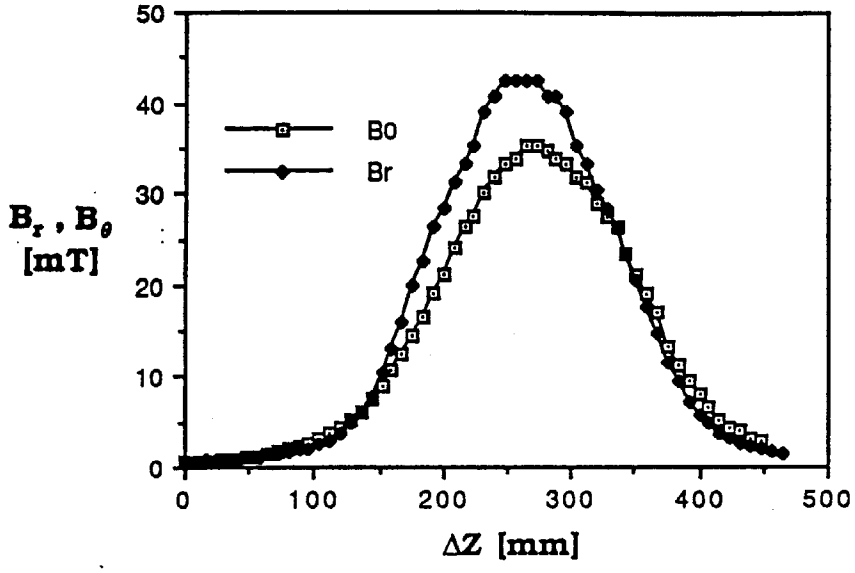

Figure 2. B_r and B_θ vs Axial position ΔZ

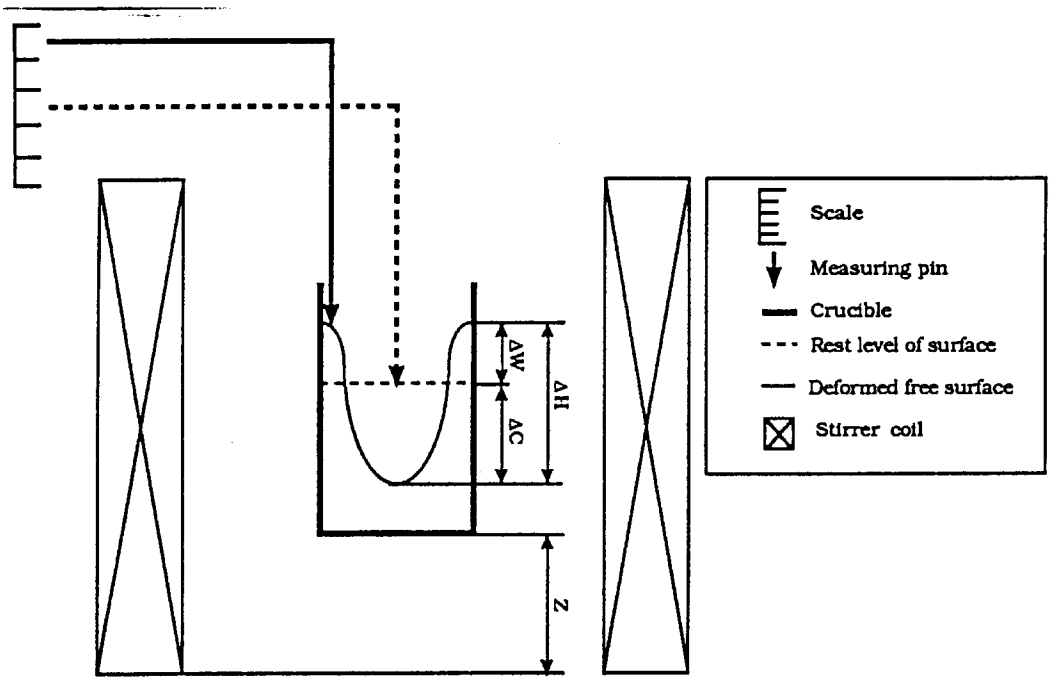

Figure 3. Measurement technique and physical meaning of ΔC,ΔW,ΔH and Z

Figure 4 shows the free surface deformation as a function of the radial component of the magnetic flux density. The magnitude of B_r is varied by changing the frequency of the coil current. As can be expected, the turbulent melt velocity should vary roughly linearly with the magnetic flux density. As a result, one would expect the free surface deformation to scale as $\sim B_r^n$, where the exponent $n > 1$. However, this is contrary to experimental observations, primarily due to the following reasons: (i) the presence of an electrically non-conducting oxide scale on the surface which tends to retard the surface

velocities, (ii) the axial gradients in the magnetic flux density as shown in Figure 2, which imply that the effective magnetic field strength is actually smaller in magnitude, and (iii) the formation of a semi-solid zone near the melt surface due to rapid cooling from the top surface, with an increase in the effective viscosity due to localized shear-thinning behavior.

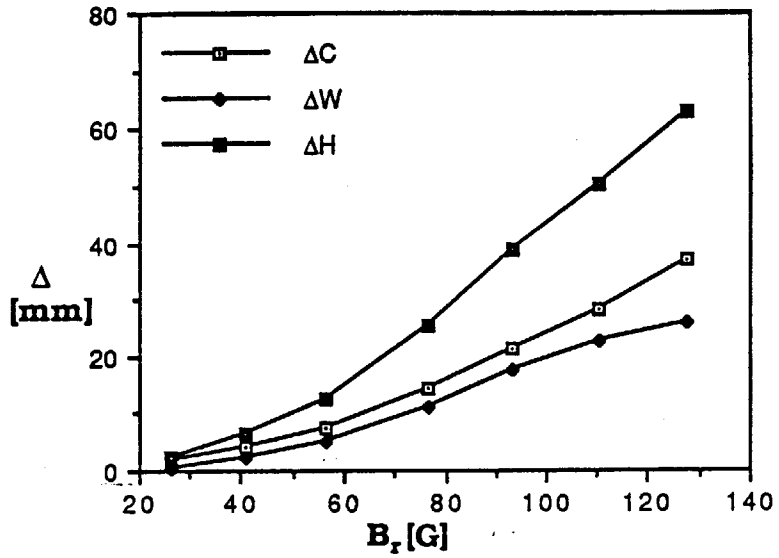

Figure 4. Free surface deformation Δ as a function of magnetic field strength

Figure 5 shows the free surface deformation dependence on the frequency of applied coil current (f). It is seen that the dependence is linear; it has been shown that $F_\theta \sim f$, and because the turbulent azimuthal velocity scales as $u_\theta \sim F_\theta^{1/2} \sim f^{1/2}$, and the free surface deformation should scale as $\Delta H \sim f$. This order of magnitude relationship is rather simplistic because in reality for the experimental conditions employed the magnetic field strength is not independent of f, i.e., $F_\theta \sim B(f) \times f$, and this would imply a dependence of the free surface deformation of the type $\Delta H \sim f^n$, where the exponent $n > 1$.

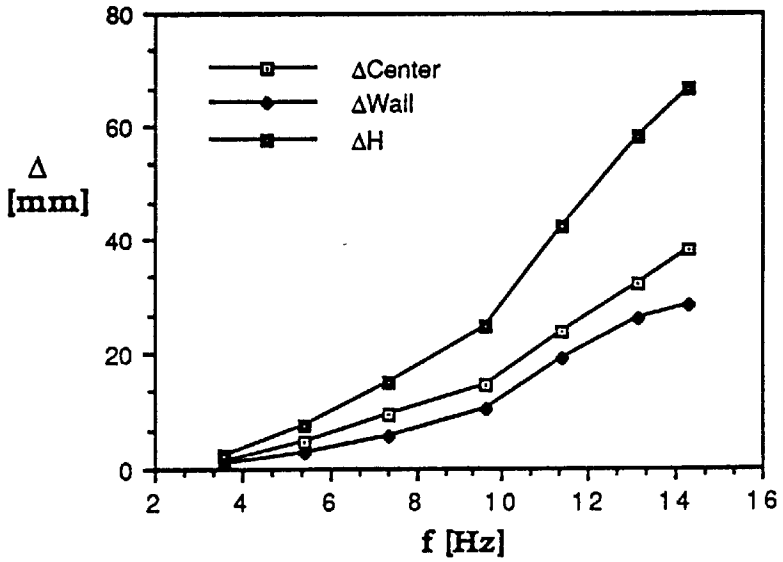

Figure 5. Frequency vs free surface deformation

Figure 6 shows the dependence of the free surface deformation on stirrer power at two different frequencies (f_1 = 14 Hz and f_2 = 9.5 Hz). Here it can be seen that the difference $\Delta H_{f1} - \Delta H_{f2}$ is fairly constant, which is expected.

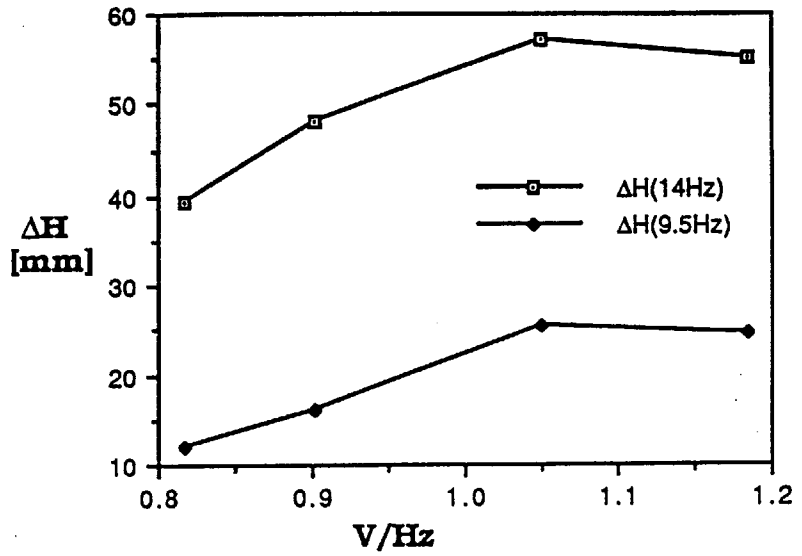

Figure 6. ΔH vs V/Hz at frequencies 14Hz and 9.5 Hz

Figure 7 shows the free surface deformation as a function of the axial position. The dependence of the free surface deformation is similar to the variation of the magnetic flux density with relative axial position. The maximum value of ΔH corresponds to the maximum effective value of B for the placement of the stirrer. The axial position Z has been defined in Figure 3.

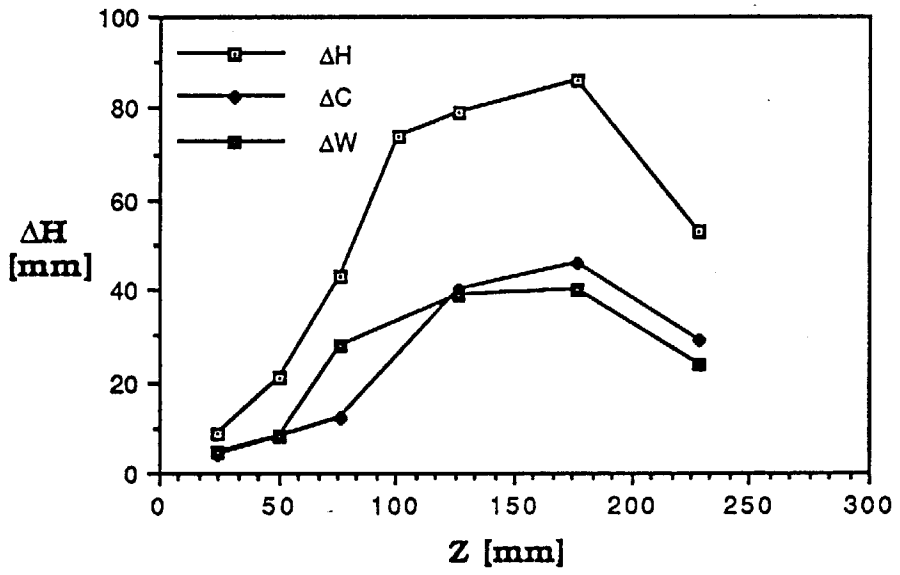

Figure 7. Free surface deformation vs axial position Z of the crucible

Figure 8 shows the computed velocity vectors in the on a z-plane at three different axial positions, at a time of 2.5 seconds. The predominant velocity is in the azimuthal direction, and it drops sharply in the near-wall region. It is also seen that for higher axial positions ($z^* = z/H$), where H is the crucible height, the

liquid is depleted near the center of the crucible and these regions now represent gaps or pockets occupied by the ambient gas.

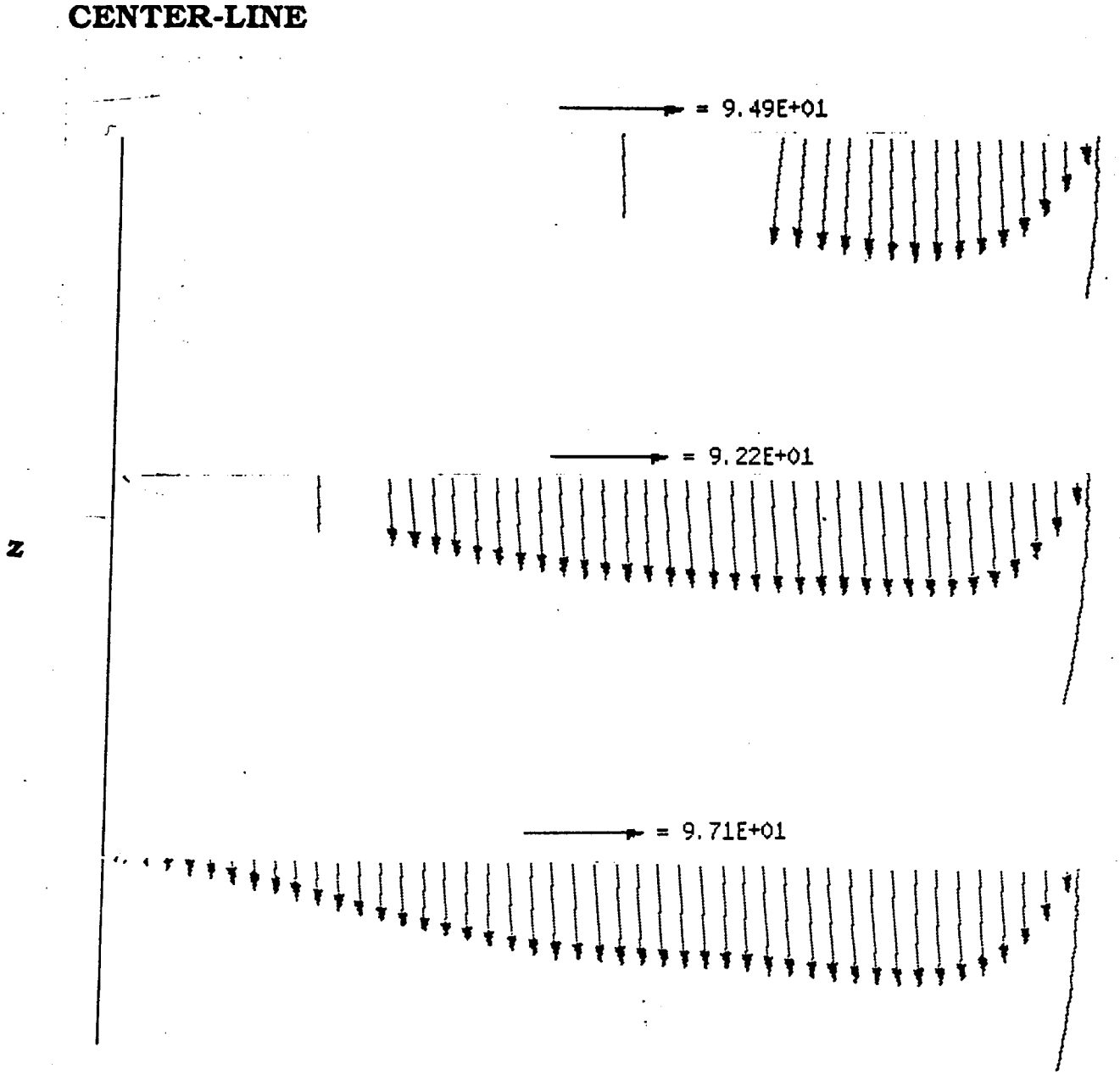

Figure 8. Calculated tangential velocities u [cm/s] at different heights z [cm] within the crucible at 2.5 s.

Figure 9 compares the measured and computed values of the free surface shape. It is seen that the experimental and predicted shapes match quite well in spite of inherent limitations of the computational procedure and the simplifying assumptions made in this analysis. The slight over-prediction is attributable to the fact that the magnitude of the magnetic flux density used is the maximum value B_{max} rather than an average value over the axial length of the crucible, and also because the theoretical model fails to take into account the surface dross

and the partially-solid layer at the surface due to rapid removal of heat through the top of the crucible.

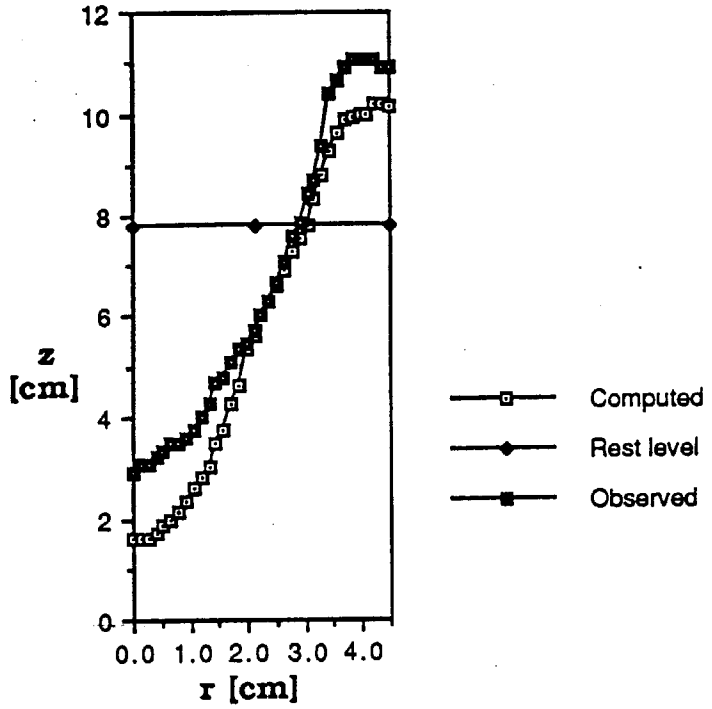

Figure 9. Computed and measured free surfaces

The free surface velocities measured with high-speed video photography as a function of time are plotted for two different axial locations of the crucible in Figure 10. It can be seen that the the surface velocity is a strong function of the axial location and hence the effective magnetic flux density. It is also seen that the velocity 'transient' is larger (~ 4 seconds) for the axial position corresponding to the lower B-value, whereas it is ~ 1 second for the higher magnetic field. This shows that the the higher electromagnetic force densities in the latter case tend to decrease the transient, which is expected. It is important to evaluate these transients for the purpose of oscillatory stirring to optimize the stirring cycles [10].

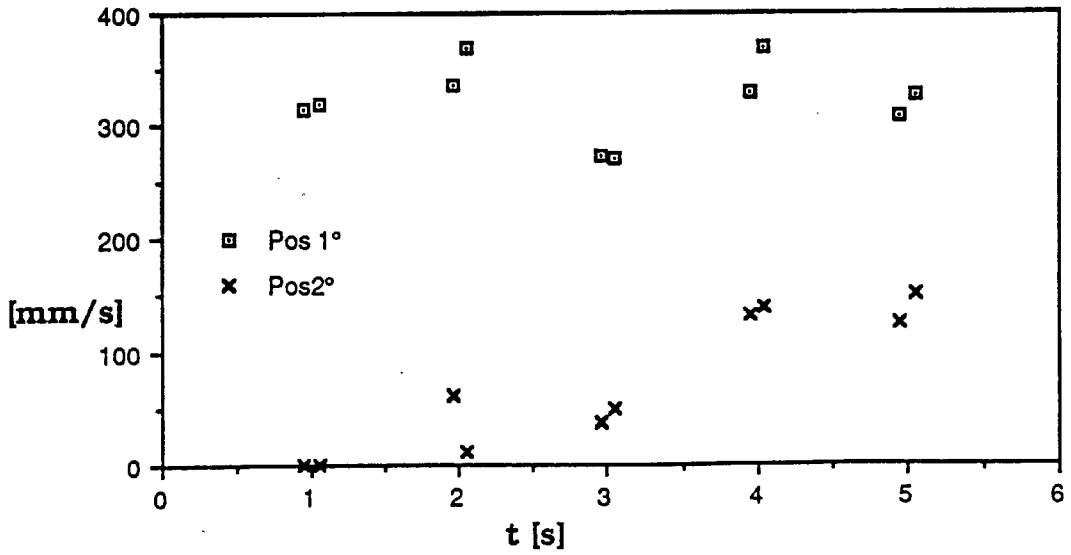

Figure 10. Surface velocities at two different crucible locations

Conclusion

A laboratory scale electromagnetic stirring system and a theoretical model capable of predicting large free surface deformations was presented. The results of the calculations were found to agree well with the observations made on the laboratory set-up.

Free surface deformation was also studied at low frequencies. The free surface deformation was found to increase almost linearly with an increase of the magnetic field strength.

Experimentally observed surface velocities were found to be considerably lower than the calculated melt velocities due to surface tension and oxide formation on the surface. Consequently, to measure the bulk flow velocities, electromagnetic probes or other immersed recording methods need to be adopted.

Acknowledgements

The theoretical modeling was done under the sponsorship of the National Science Foundation (Grant No. MSM-86-11879).

References

[1] S. Asai, *Recent activities and trend of electromagnetic processing of materials*, Proc. of 6th Int. Iron and Steel Congress, pp 370-379, 1990, Nagoya, ISIJ.

[2] M. Garnier, *Basis and application of electromagnetic processing of liquid materials*, Proc. of 6th Int. Iron and Steel Congress, pp 226-238,1990, Nagoya, ISIJ.

[3] L. Beitelman, J.A. Mulcahy: *Influence of electromagnetic stirring on quality of continuously cast billets*, Continuous casting of steel, Conf. Proc of the 2nd process technology conference, Vol 2, Chicago meeting, Feb 23-25, 1981, pp 270-277 AIME 1981.

[4] J.L.Meyer: *Electromagnetic processes in aluminum cast house and foundries: an overview*, Magnetohydrodynamics, in process metallurgy Ed. J. Szekely, J. Evans, K. Blazek and El-Kaddah, TMS, pp 127-143,1991.

[5] R.Moreau: *Magnetohydrodynamics*, Kluwer Academic Publisher, Dordrect, the Netherlands, 1990.

[6] J.A. Shercliff: *A textbook of magnetohydrodynamics*, Pergamon, 1965.

[7] W.F. Hughes,F.J. Young: *Electromagnetodynamics of fluids*, John Wiley & Sons, Inc, NY, NY, USA, 1966.

[8] J. Szekely,J. Evans. K. Blazek and El-Kaddah ed. *Magnetohydrodynamics in Process Metallurgy* , TMS,1991.

[9] N. Saluja, Sc.D. Thesis, Dept. of Mat. Sci. and Eng., Massachusetts Institute of Technology, 1991.

[10] N. Saluja, O.J. Ilegbusi and J.Szekely, *Three dimensional flow and free surface phenomena in electromagnetically stirred molds in continuous casting*, Proc. of the 6th international iron and steel congress Vol. 4, Oct.21-26.1990, pp 659-666, Nagoya congress center, Nagoya, Japan, ISIJ 1990.

[11] N. Saluja, O. Ilegbusi, and J. Szekely, *Fluid flow phenomena in the electromagnetic stirring of continuous casting systems, part 1: the behavior of a cylindrically shaped laboratory scale installation*, Steel Research, No. 10/90, pp. 455-466, 1990.

[12] N. Saluja, O.J. Ilegbusi and J. Szekely, *On the calculation of the electromagnetic force field in the circular stirring of metallic melts*, accepted for publication, 1992.

[13] O.J. Ilegbusi and J. Szekely, *Three-dimensional velocity fields for newtonian and non-newtonian melts produced by a rotating magnetic field*, ISIJ International, Vol. 29, No. 6, 1989.

[14] W. Rodi: *Turbulence models and their application in hydraulics*, Int. Ass. for hydraulic research, The Netherlands, 1984.

[15] B.E. Launder and D.B. Spalding, *The numerical computation of turbulent flows*,Computer methods in applied mechanics and engineering, 3, (1974),pp. 269-289.

[16] Karl-Heinz Spitzer, Mathias Dubke, Klaus Schwerdtfeger, *Rotational Electromagnetic Stirring in continuous casting of round strands*, Metall. Trans B Vol 17B, March 1986, pp 119-131.

[17] C.W. Hirt, B.D. Nichols: *Volume of fluid (VOF) method for the dynamics of free boundaries*, J. Comp. Phys. Vol 39, pp 201, 1981.

[18] P.L. Conley, J.L. Kirtley, Jr., W.H. Hagman, and A.H.M.S. Ula, Demonstration of a Helical Armature for a Superconducting Generator, IEEE PES Summer Meeting, Vancouver, British Columbia, Canada, 1979.